Received: 8 September 2022 | Revised: 25 October 2022 | Accepted: 26 October 2022

DOI: 10.1002/pro.4485

FULL-LENGTH PAPER

THE PROTEIN SOCIETY WILEY

Signal peptide stabilizes folding and inhibits misfolding of serum amyloid A

Jin-Lin Wu[1,2] | **Yun-Ru Chen**[1,2]

[1]Ph.D. Program for Cancer Biology and Drug Discovery, China Medical University and Academia Sinica, Taichung, Taiwan

[2]Genomics Research Center, Academia Sinica, Taipei, Taiwan

Correspondence
Yun-Ru Chen, Genomics Research Center, Academia Sinica, 128, Academia Rd, Section 2, Nankang District, Taipei 115, Taiwan.
Email: yrchen@gate.sinica.edu.tw

Funding information
Academia Sinica, Taiwan, Grant/Award Number: AS-CFII-108-119

Review Editor: Aitziber L. Cortajarena

Abstract

Signal peptide (SP) plays an important role in membrane targeting for insertion of secretory and membrane proteins during translocation processes in prokaryotes and eukaryotes. Beside the targeting functions, SP has also been found to affect the stability and folding of several proteins. Serum amyloid A (SAA) proteins are apolipoproteins responding to acute-phase inflammation. The fibrillization of SAA results in a protein misfolding disease named amyloid A (AA) amyloidosis. The main disease-associated isoform of human SAA, SAA1.1, is expressed as a precursor protein with an N-terminal signal peptide composed of 18 residues. The cleavage of the SP generates mature SAA1.1. To investigate whether the SP affects properties of SAA1.1, we systematically examined the structure, protein stability, and fibrillization propensity of pre-SAA1.1, which possesses the SP, and Ser-SAA1.1 without the SP but containing with an additional N-terminal serine residue. We found that the presence of the SP did not significantly affect the predominant helical structure but changed the tertiary conformation as evidenced by intrinsic fluorescence and exposed hydrophobic surfaces. Pre-SAA1.1 and Ser-SAA1.1 formed distinct oligomeric assemblies in which pre-SAA1.1 populated as tetramer and octamer, whereas Ser-SAA1.1 existed as a predominant hexamer. Pre-SAA1.1 was found significantly more stable than Ser-SAA1.1 upon thermal and chemical unfolding. Ser-SAA1.1, but not pre-SAA1.1, is capable of forming amyloid fibrils in protein misfolding study, indicating a protective role of the SP. Altogether, our results demonstrated a novel role of the SP in SAA folding and misfolding and provided a novel direction for therapeutic development of AA amyloidosis.

KEYWORDS
AA amyloidosis, folding, misfolding, serum amyloid A, signal peptide, stabilization

1 | INTRODUCTION

A signal peptide (SP) is a short segment normally resided at the N-terminus of newly synthesized polypeptides for secretory pathways. Both prokaryotic and eukaryotic proteins rely on SPs to direct them to the target sites for

Abbreviations: AA, amyloid A; ANS, 8-anilino-1-naphthalenesulfonic acid; AUC, analytical ultracentrifugation; CD, circular dichroism; DMSO, dimethyl sulfoxide; DTT, dithiothreitol; IAEW, intensity-averaged emission wavelength; PICUP, photoinduced crosslinking of unmodified proteins; SAA, serum amyloid A; SP, signal peptide; TEM, transmission electron microscopy; ThT, thioflavin T; UV, ultraviolet.

cytoplasmic transportation. The process of protein transportation typically involves targeting to and translocating across one or several membrane bilayers.[1,2] Most of the secretory proteins are synthesized as precursors, that is, pre-proteins with an additional N-terminal sequence served as SP. SPs are highly variable in length. They usually consist of 15 to >50 amino acids and share low primary sequence homology.[3,4] SPs possess a typical characteristic tripartite pattern: a positively charged N-terminus (N-region), a central region composed of 7–15 hydrophobic residues (H-region), and a more polar C-terminal domain containing the signal peptidase cleavage site (C-region).[5] In eukaryotic cells, most secretory proteins are co-translationally translocated to endoplasmic reticulum (ER).[6] Some proteins can also enter ER post-translationally.[7] The signal recognition particle recognizes and binds to SP of a newly synthesized protein, and targets the nascent protein to ER.[8] After or during translocation, SP are then removed by the signal peptidase complex.[8]

Earlier studies on SPs focused on their direct interaction with membrane for protein insertion to or across the membrane. Later, some studies reported the involvement of SPs in folding of precursor proteins. It has been shown that the presence of SP leads to folding retardation of *Escherichia coli* (*E. coli*) precursor maltose binding protein (preMBP) when compared with the corresponding mature protein (MBP).[9,10] Thermodynamic studies further demonstrated that preMBP has a reduced stability in comparison with MBP.[11] The slow folding and destabilization caused by the SP likely maintain MBP in an unfolded, translocation-competent conformation and thus facilitate the interactions between the protein and the translocation machinery.[11] Other studies on *E. coli* MBP and thioredoxin both showed that the presence of SP reduces the protein activity and increases the aggregation propensity of the proteins.[12,13] In contrast to MBP, propeptide of caspase-3 has been shown to facilitate the reassembly of caspase-3 and stabilize the native structure, but not to change the assembly.[14,15]

Serum amyloid A (SAA) refers to a highly conserved family of proteins involved in multiple biological processes including cholesterol transport and various immunological responses. Recently, it has also been reported being associated with several cancers.[16–21] SAA is mainly produced by hepatocytes and secreted into blood.[22] Among four family members, SAA1 and SAA2 are acute-phase proteins which are known as acute-phase SAA (A-SAA).[23] Upon inflammatory responses, the blood level of A-SAA elevates significantly up to 1,000-fold when compared with the basal level.[24] Prolonged high level of A-SAA associated with chronic inflammation sometimes leads to a systemic disorder called amyloid A (AA) amyloidosis.[24] AA amyloidosis is characterized by extracellular accumulation and deposition of insoluble amyloid fibrils derived from misfolded SAA proteins. Previous studies have revealed that human SAA1, specifically SAA1.1 (also known as SAA1α), is the predominant component of AA amyloid deposits.[25,26] During synthesis in liver cells, SAA1.1 is expressed as a precursor protein (pre-SAA1.1) which consists of 122 amino acids including a SP with 18-residues at the N-terminus (Figure 1a).[27] This SP directs pre-SAA1.1 to the ER, and is cleaved prior to the extracellular secretion of the mature SAA1.1 (104 amino acid residues).[28] The crystal structure of mature human SAA1.1 revealed that monomeric SAA1.1 forms a cone-shaped four-helix bundle stabilized by a relatively unstructured C-terminal tail (Figure 1b).[29] This study also showed that SAA1.1 monomers can assemble into a hexamer consisting of two trimers (Figure 1b). The trimeric SAA1.1 is packed by subunits A, B, and C of SAA1.1 monomers in a head-to-tail arrangement. The stabilization of the trimer involves a combination of hydrogen bonds, salt bridges, and hydrophobic interactions formed mainly by residues from the first α-helix. Two trimers form hexameric SAA1.1 through the interactions at the large hydrophobic interface. The hydrophobic face of each trimer is buried at this dimer interface and the hydrophilic face is exposed to the solvent (Figure 1C). Low conservation of the residues at the dimer and trimer interface of the SAA1.1 hexamer among different species suggests that different SAA proteins likely form distinct oligomers.[29,30]

To elucidate the folding and misfolding mechanisms of SAA and AA amyloidosis as well as the effect of the SP on SAA, in the present study we investigated the role of the SP in pre-SAA1.1. We first used multiple biophysical methods including far-UV circular dichroism (CD), fluorescence spectroscopy, analytical ultracentrifugation (AUC), photoinduced crosslinking of unmodified proteins (PICUP), and temperature and chemical denaturation to examine folding properties of pre-SAA1.1 and SAA1.1. Then, the misfolding properties of pre-SAA1.1 and SAA1.1 were further examined by thioflavin T (ThT) assay and transmission electron microcopy (TEM). Our results revealed a stabilization role of SP in SAA and provided a potential therapeutic target for amyloid fibril formation of SAA and AA amyloidosis.

2 | RESULTS

2.1 | Pre-SAA1.1 and Ser-SAA1.1 adopt helical structures

To improve the efficiency of his-tag removal from SAA1.1 protein during the purification, a complete TEV cleavage

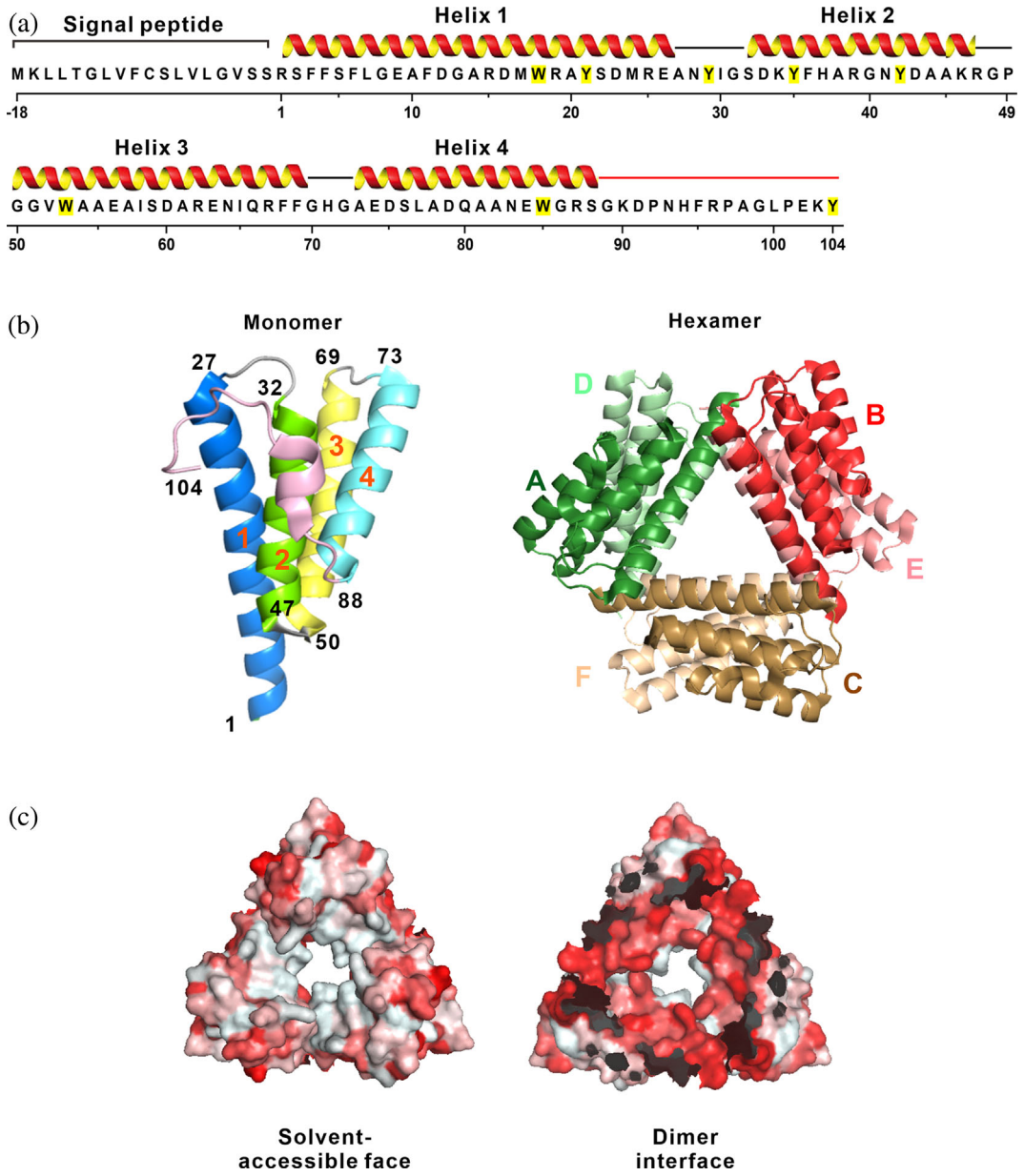

FIGURE 1 Primary sequence and structure of human SAA1.1. (a) Primary sequence and secondary structure of human SAA1.1. The helices and lines above the sequence indicate α-helices and loops, respectively. The 18-residue signal peptide is indicated. Tyrosine and tryptophan residues are shaded in yellow. (b) Cartoon representation of the crystal structure of monomeric and hexameric human SAA1.1. The figures were generated by PyMOL using PDB code 4IP8 and 4IP9 for monomer and hexamer, respectively.[29] The four α-helices of the monomer are indicated in blue (helix 1, residues 1–27), green (helix 2, residues 32–47), yellow (helix 3, residues 50–69), and cyan (helix 4, residues 73–88) and the C-terminal tail (residues 89–104) is colored in pink. (c) The hydrophobicity of the two surfaces on SAA1.1 trimer. The hydrophobic residues are indicated in red and the shades of color are based on the hydrophobicity scale[65]

site sequence ENLYFQS was inserted between His-tag and the mature SAA1.1. Therefore, our purified SAA1.1 possesses an additional serine residue at the N-terminus and is so referred to as Ser-SAA1.1 to distinguish it from the natural human SAA1.1. To understand the influence of the SP on the conformation of SAA1.1, we first characterized the secondary structures of pre-SAA1.1 and Ser-SAA1.1. Pre-SAA1.1 and Ser-SAA1.1 at 20 μM were subjected to far-UV CD spectroscopy. Both pre-SAA1.1 and Ser-SAA1.1 displayed spectra with two minima at 208 and 222 nm, which is characteristics of α-helical proteins (Figure 2a). The spectra were then subjected to secondary structure prediction by K2D3.[31] The prediction showed that pre-SAA1.1 possessed 83.13% α-helices and 0.29% β-strands, and Ser-SAA1.1 possessed 92.33% α-helices and 0.13% β-stands. This result is consistent

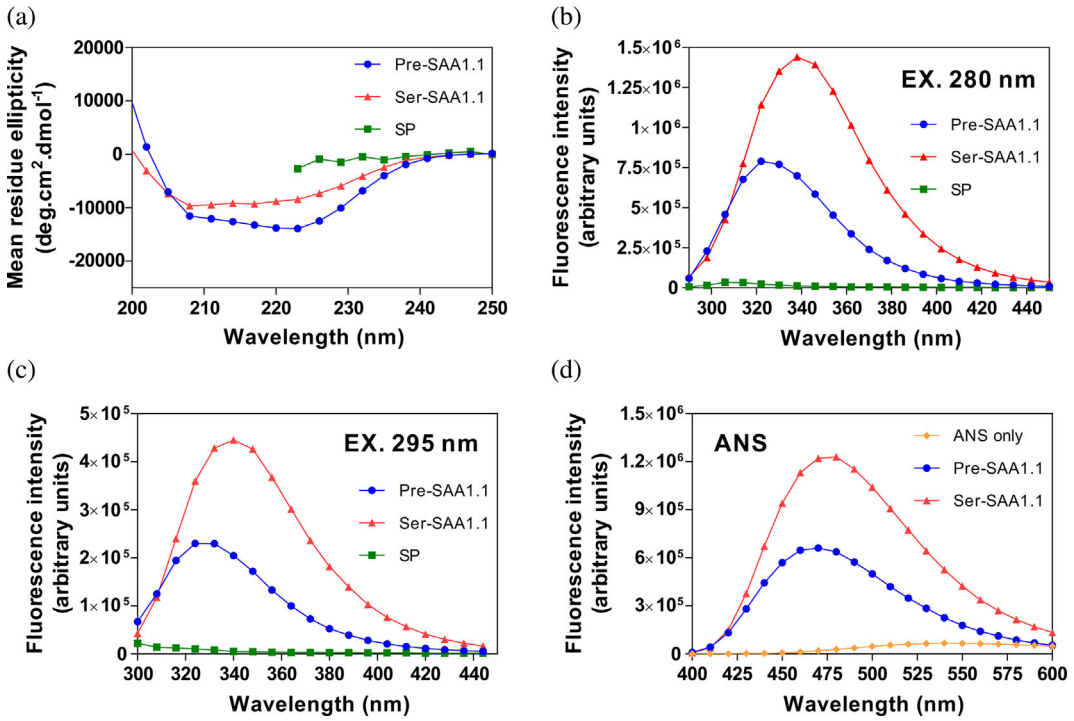

FIGURE 2 Far-UV CD and fluorescence spectra of pre-SAA1.1 and Ser-SAA1.1. All the spectroscopic measurements were conducted on 20 μM pre-SAA1.1 (blue circle), Ser-SAA1.1 (red triangle), and synthetic SP (green square) in 50 mM sodium phosphate buffer, at pH 7.0. (a) Far-UV CD spectra of pre-SAA1.1 and Ser-SAA1.1. (b) Intrinsic fluorescence spectra of pre-SAA1.1 and Ser-SAA1.1 with an excitation wavelength at 280 nm. (c) Intrinsic fluorescence spectra of pre-SAA1.1 and Ser-SAA1.1 with an excitation wavelength at 295 nm. (d) ANS binding of pre-SAA1.1 and Ser-SAA1.1. ANS at 200 μM was added into the protein samples. The ANS fluorescence was excited at 375 nm

with the previous study that showed crystallized monomeric human SAA1.1 has an all-helical structure without detectable β-strands.[29] Our far-UV CD result indicated that the presence of SP did not change the helical conformation of SAA1.1. We also examined the secondary structure of 20 μM synthetic SP alone. Due to the presence of DMSO, the spectrum of SP cannot be further measured below 222 nm. However, the spectra showed that SP did not possess significant secondary structure.

2.2 | The presence of the SP results in an altered tertiary structure of SAA1.1

Next, we employed intrinsic and 8-anilino-1-naphthalenesulfonic acid (ANS) fluorescence spectroscopy to examine the tertiary structures of pre-SAA1.1 and Ser-SAA1.1. Human SAA1.1 possesses three tryptophan residues, that is, Trp18, Trp53, and Trp85, in helix 1, 3, and 4, respectively, and five tyrosine residues, that is, Tyr21, Tyr29, Tyr35, Tyr42, and Tyr104, mainly within helix 1 and 2 (Figure 1a). No tryptophan and tyrosine are in the SP region. The proteins were excited at 280 or 295 nm for intrinsic fluorescence. The fluorescence spectrum of pre-SAA1.1 excited at 280 nm displayed a fluorescence emission maximum (F_{max}) at ~324 nm with lower quantum yield when compared with the F_{max} of Ser-SAA1.1 at ~337 nm (Figure 2b). When excited at 295 nm, pre-SAA1.1 showed a F_{max} at ~328 nm whereas the F_{max} of Ser-SAA1.1 located at ~338 nm (Figure 2C). In comparison with Ser-SAA1.1, the blue-shifted F_{max} of pre-SAA1.1 suggests that the tryptophan residues in pre-SAA1.1 are in a more hydrophobic environment, possibly been buried. This result showed that the presence of SP changes the tertiary structure of SAA1.1. We further performed ANS binding assay to examine the exposed hydrophobic clusters on pre-SAA1.1 and Ser-SAA1.1. ANS is a fluorescent dye that preferentially binds to the exposed hydrophobic clusters of proteins and results in an increased fluorescence quantum yield and a blue-shifted emission wavelength.[32–34] While free ANS excited at 375 nm emitted fluorescence at ~540 nm with a low quantum yield, the ANS fluorescence spectra of pre-SAA1.1 and Ser-SAA1.1 showed an increased quantum yield and the F_{max} blue-shifted to ~469 and ~475 nm, respectively, indicating the binding of ANS to both pre-SAA1.1 and Ser-SAA1.1 (Figure 2D). Ser-SAA1.1 showed higher ANS fluorescence intensity compared with pre-SAA1.1 suggesting a difference in their exposed hydrophobic surfaces.

2.3 | Pre-SAA1.1 and Ser-SAA1.1 possess distinct assemblies

Previous crystal structure study demonstrated that SAA1.1 associates into a hexameric structure in a crystallization condition (30% [wt/vol] PEG 2000 monomethyl ether, 0.1 M Tris, pH 8.5, and 0.2 M trimethylamine N-oxide).[29] The study also showed that SAA1.1 oligomerizes as a hexamer in a buffer containing 10 mM HEPES, pH 7.4, and 150 mM NaCl. Our tryptophan fluorescence studies showed that the tryptophan residues of pre-SAA1.1 are buried in a more hydrophobic environment, suggesting that pre-SAA1.1 and Ser-SAA1.1 may possess different assemblies. To further examine the assembly of pre-SAA1.1 and Ser-SAA1.1 in solution, SV-AUC was employed (Figure 3). Pre-SAA1.1 and Ser-SAA1.1 at 20 μM in 50 mM sodium phosphate buffer, pH 7.0, were subjected to SV-AUC experiments at 4°C. The data were analyzed and fitted. Our pre-SAA1.1 and Ser-SAA1.1 have theoretical molecular weights of 16,260 and 11,771 Da, respectively. For pre-SAA1.1, the result showed two similar intensity peaks, one at 4.83 S and the other at 7.98 S, representing molecular masses of ~64 kDa as pre-SAA1.1 tetramer and ~128 kDa, as pre-SAA1.1 octamer, respectively. For Ser-SAA1.1, the result showed a single peak at 3.06 S representing a molecular mass of ~72 kDa as Ser-SAA1.1 hexamer. This result is consistent with the previous study that demonstrated SAA1.1 existing mainly as a hexamer in solution.[29] The SV-AUC results indicated that pre-SAA1.1 and Ser-SAA1.1 in solution form different oligomeric assemblies. Since there is a cysteine residue in the SP region, it is possible that two pre-SAA1.1 form intermolecular disulfide bonds in the non-reducing phosphate buffer. To investigate whether there is formation of disulfide bond, we performed AUC on pre-SAA1.1 in the phosphate buffer containing 3 mM DTT. Under the reducing condition, pre-SAA1.1 showed two peaks with similar intensities, one at 4.83 S and the other at 8.97 S, representing molecular masses of ~63 kDa as pre-SAA1.1 tetramer and ~136 kDa, as pre-SAA1.1 octamer, respectively (Figure S1). The result suggested that there is no disulfide bond formation in pre-SAA1.1.

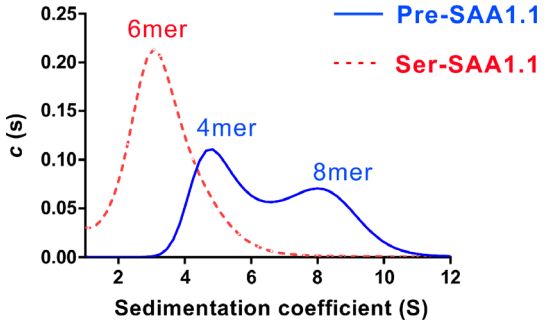

FIGURE 3 Assembly of pre-SAA1.1 and Ser-SAA1.1 analyzed by AUC. The assembly of pre-SAA1.1 and Ser-SAA1.1 was analyzed at a protein concentration of 20 μM in 50 mM sodium phosphate buffer, pH 7.0, by SV-AUC. Sedimentation coefficient distributions adopted from AUC for pre-SAA1.1 (blue) and Ser-SAA1.1 (red) are shown. The calculated assemblies are indicated

Next, we employed PICUP assay to crosslink the assemblies and detected the species by western blot (Figure 4). PICUP assay is a photo-crosslinking assay that has been used to examine amyloid-β (Aβ) in Alzheimer disease.[35–39] The protein samples with or without the photosensitive dye $Ru(bpy)_3Cl_2$ were subjected to light irradiation for different lengths of time, from 0 to 30 s, then subjected to SDS-PAGE for Western blot. Our results showed that pre-SAA1.1 monomer migrated at ~15 kDa which is consistent with the theoretic molecular mass of pre-SAA1.1 (~16.3 kDa) in Western blot. The results also showed that pre-SAA1.1 possessed dimer species even in the reducing condition without crosslinking, while with the increase of irradiation time pre-SAA1.1 formed dimer, trimer, tetramer, pentamer, and high-molecular-weight species. For Ser-SAA1.1, the monomer migrated at ~9 kDa which is smaller than the theoretic molecular mass of Ser-SAA1.1 (~11.8 kDa) in western blot. This faster migration of Ser-SAA1.1 in SDS-PAGE may be due to protein hydrophobicity. Based on the migration of Ser-SAA1.1 around 9 kDa in SDS-PAGE, the crosslinking result showed that Ser-SAA1.1 may form a dimer, trimer, tetramer, pentamer, hexamer, heptamer, octamer, and high-molecular-weight species. Although the exact molecular mass is difficult to interpret, the band indicating trimeric Ser-SAA1.1 was more abundant in the short crosslinking time, such as 1 s, which may suggest a dominant trimeric species of Ser-SAA1.1. This result is consistent with SV-AUC result showing that pre-SAA1.1 and Ser-SAA1.1 form different assemblies and the building units may be different. Altogether, our results demonstrated that the presence of SP affects the oligomerization process and assembly of SAA1.1.

2.4 | The presence of SP stabilizes SAA1.1

To investigate the effect of the SP on SAA1.1 stability, we performed temperature-induced denaturation. Unfolding of pre-SAA1.1 and Ser-SAA1.1 was induced by melting from 4°C to 100°C and refolding by cooling from 100°C to 4°C. The conformational changes were automatically monitored by far-UV CD at 222 nm. The data were collected, normalized, and plotted against temperature for

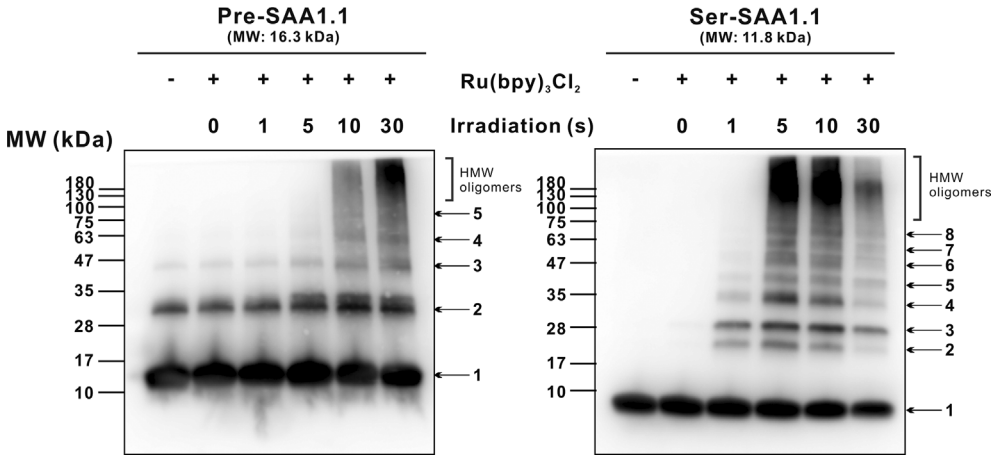

FIGURE 4 Assembly of pre-SAA1.1 and Ser-SAA1.1 crosslinked by PICUP. The assembly of pre-SAA1.1 and Ser-SAA1.1 was analyzed at a protein concentration of 20 μM in 50 mM sodium phosphate buffer, pH 7.0, by PICUP. Pre-SAA1.1 and Ser-SAA1.1 samples with or without PICUP were subjected to western blot probed by an anti-SAA antibody. The possible assemblies of pre-SAA1.1 and Ser-SAA1.1 are indicated by arrows and numbers. HMW, high-molecular-weight

melting curves. The melting curve showed that pre-SAA1.1 was 50% unfolded with Tm at ~48°C and fully unfolded at ~80°C (Figure 5a). By contrast, Ser-SAA1.1 was 50% unfolded with Tm at ~23°C and fully unfolded at a much lower temperature, ~35°C. The relative low melting temperatures may suggest a marginal stability for SAA1.1 in physiological temperature. When cooling from 100°C back to 4°C, the signal of pre-SAA1.1 was found to be irreversible, suggesting that there was no refolding for pre-SAA1.1 and the conformation of pre-SAA1.1 remained fully unfolded. In contrast to pre-SAA1.1, Ser-SAA1.1 showed better thermo-reversibility with approximately 80% signal recovered after cooling (Figure 5a). The CD spectra of native and refolded pre-SAA1.1 and Ser-SAA1.1 at 4°C were also shown to depict the reversibility (Figure 5b). The results indicated that the SP increases the thermal stability of SAA1.1 but affects the reversibility.

We also examined the stability of pre-SAA1.1 and Ser-SAA1.1 by chemical denaturation and the changes in secondary and tertiary structure were monitored by far-UV CD and intrinsic fluorescence spectroscopy upon urea unfolding (Figure S2). The fluorescence intensity averaged emission wavelengths (IAEW) were calculated from the fluorescence spectra and plotted against urea concentration. The far-UV CD and intrinsic fluorescence spectra of native and unfolded pre-SAA1.1 and Ser-SAA1.1 are shown in Figure S2A,B. In the intrinsic fluorescence study, the unfolding curve of pre-SAA1.1 displayed a pattern similar to two-state folding mechanism with a transition from ~1 to 4.5 M urea (Figure S2C). The mid-point of the transition, $[Urea]_{1/2}$, was around 2.5 M. The denaturation curve obtained from far-UV CD showed a transition at higher urea concentrations from 2 to 5 M, indicating the unfolding of pre-SAA1.1 might not be cooperative. By contrast, both signals detected by fluorescence and CD for Ser-SAA1.1 showed a transition from ~0 to 3 M urea with $[Urea]_{1/2}$ around 1.5 M and without an obvious pre-transition state (Figure S2C). These results together with the temperature melting study showed that Ser-SAA1.1 is less stable than pre-SAA1.1 demonstrating the role of SP in stabilizing SAA1.1.

2.5 | SP in pre-SAA1.1 inhibits fibrillization

To examine whether the SP affects the amyloidogenic property of SAA1.1, we employed ThT binding assay to monitor the amyloid fibrillization of pre-SAA1.1 and Ser-SAA1.1 (Figure 6a). ThT is a classic amyloid dye that binds to the cross-β structure of amyloid fibrils.[40,41] Pre-SAA1.1 and Ser-SAA1.1, and a SP control were subjected to ThT assay at 25°C with 40-s agitation every 30 min. The results showed that only Ser-SAA1.1 exhibited ThT fluorescence enhancement as a function of time, indicating a spontaneous fibrillization (Figure 6a). No increase in ThT fluorescence was detected for pre-SAA1.1 and the SP control throughout the measurement. This indicated that pre-SAA1.1 and SP alone was unable to form amyloid fibrils. In addition, we added equimolar synthetic SP to Ser-SAA1.1 to examine the effect of SP in *trans*. The results showed that Ser-SAA1.1 in the presence of the external SP was still capable of forming amyloid fibrils in similar fashion and kinetics (Figure 6a). However, we have noticed that the ThT binding curve of Ser-SAA1.1 in

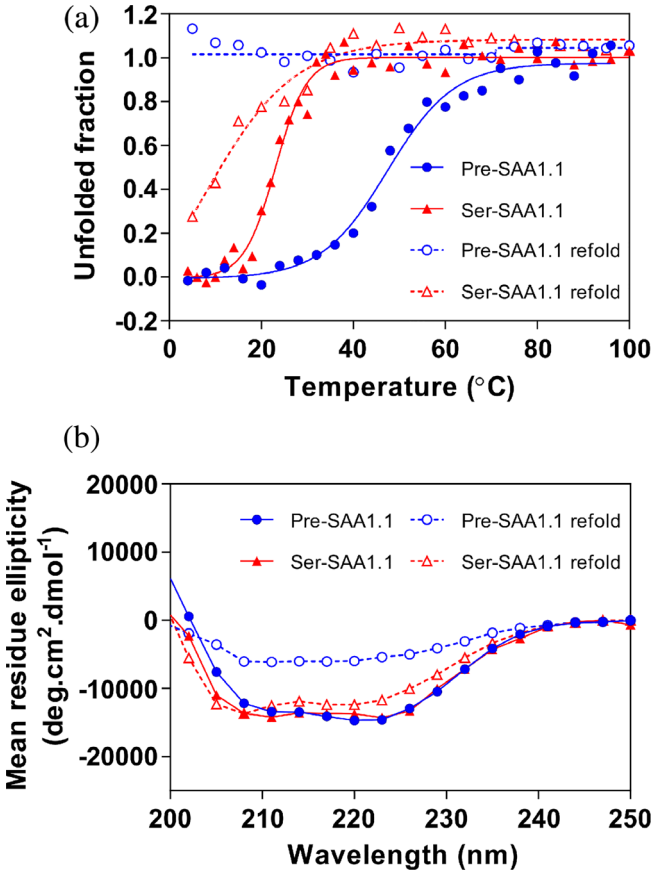

FIGURE 5 Thermostability of pre-SAA1.1 and Ser-SAA1.1. Thermal denaturation was performed on 20 μM pre-SAA1.1 and Ser-SAA1.1 in 50 mM sodium phosphate buffer, pH 7.0. (a) Temperature melting and refolding curves of pre-SAA1.1 (blue circle) and Ser-SAA1.1 (red triangle). Temperature melting was labeled as solid symbols and refolding as empty symbols. The signals were normalized to indicate unfolded fraction (0 represents the native state and 1 the unfolded state). Curves are only presented to show the data trends. (b) CD spectra of native and refolded pre-SAA1.1 and Ser-SAA1.1 at 4°C. Pre-SAA1.1 and Ser-SAA1.1 are indicated as blue circles and red triangles, respectively. Native and refolded proteins are labeled as solid symbols and empty symbols, respectively

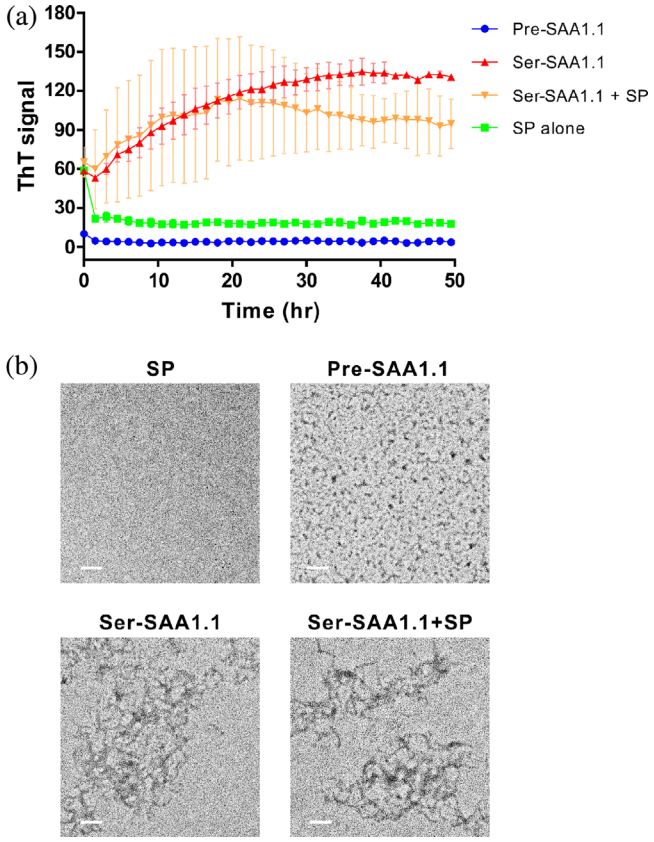

FIGURE 6 Amyloidogenicity of pre-SAA1.1 and Ser-SAA1.1. ThT assay was performed on 20 μM proteins in 50 mM sodium phosphate, pH 7.0, at 25°C with 40-s agitation every 30 min. Fibrillization kinetics was monitored by fluorescence of 10 μM ThT with excitation and emission at 442 and 485 nm, respectively. Synthetic SP was added to Ser-SAA1.1 in a molar ratio of 1:1. Symbols represent the average and error bars represent the standard deviation of three experiments. (a) Fibrillization kinetics of pre-SAA1.1 and Ser-SAA1.1 with or without the addition of the synthetic SP. (b) TEM images of the end-point products from the ThT assay (scale bars, 100 nm)

the presence of SP showed larger error bars compared with Ser-SAA1.1. This may suggest that the addition of the external SP interferes with the fibrillization process or the interaction of ThT to the fibrils. To confirm whether the addition of SP in *trans* affects quantity of the fibrils formed, we repeated the ThT assay for Ser-SAA1.1 with or without SP addition and collected the supernatants from the end-point products after centrifugation to remove fibrils (Figure S3). The supernatants were quantified by western blot and absorbance at 280 nm. The results showed similar quantities of soluble Ser-SAA1.1 remained in both samples, indicating that fibril formation was not substantially inhibited by the external SP. The morphology of the end-point products from the ThT assay was further examined by TEM. Consistent with the results of the ThT assay, the TEM images showed the presence of long fibrils in the end-point products of Ser-SAA1.1 with or without the addition of the external SP (Figure 6b). No fibril-like species were observed in pre-SAA1.1, although some small spherical aggregates were observed in the end-point product of pre-SAA1.1. Regarding the potential mis-disulfide bond formation in pre-SAA1.1, we also performed ThT assay of pre-SAA1.1 in the presence of DTT. The ThT results showed no fibril formation for pre-SAA1.1 under the reducing condition (Figure S4). Taken together, our results showed that the SP in pre-SAA1.1 inhibits the amyloid fibrillization properties of SAA1.1. Moreover, the

substantial inhibitory effect only exists when the SP *in cis* in SAA1.1 protein.

3 | DISCUSSION

AA amyloidosis is a protein misfolding disease occurring in the peripheral system,[42] that is different from many amyloidosis in the central nervous system such as Alzheimer disease, Parkinson disease, and Huntington disease.[43] SAAs, the pathogenic proteins of AA amyloidosis, form insoluble filamentous amyloids and deposit in many organs in the peripheral system,[44] where kidneys, liver, and spleen are the main sites of SAA amyloid deposition.[45] Kidney involvement is a common manifestation for AA amyloidosis and proteinuria is often the first clinical presentation of the disease.[46] For patients who have sustained high level of SAA attributed from the active inflammation diseases, the progression of AA amyloidosis can lead to severe organ failure and finally death. For example, SAA deposition in cardiac tissue leads to significant ventricular hypertrophy and abnormal cardiac wall motion.[47,48] A study showed that the estimated 5-year survival was 31.3% in AA amyloidosis patients with cardiac involvement compared with 63.3% in patients without cardiac involvement.[49] Hence, elucidating SAA folding and misfolding mechanisms is essential for therapeutic development for AA amyloidosis. Previous SAA studies mostly focused on mature SAA or SAA peptides; however, to the best of our knowledge, the precursor protein pre-SAA with the SP has never been examined. In the present study, we investigated the effect of SP on structure, stability, and aggregation property of human SAA1.1 to facilitate the understanding of fundamental folding and misfolding mechanisms of SAA and AA amyloidosis. We found that the presence of the SP did not affect the helical structure of SAA1.1 but showed apparent influences on the tertiary and quaternary structure of SAA1.1. The tryptophan residues of pre-SAA1.1 are buried in a more hydrophobic environment, indicating an altered packing of the protein molecules in comparison with Ser-SAA1.1 without SP. Consistently, pre-SAA1.1 also adopted less exposed hydrophobic surfaces compared with Ser-SAA1.1. Both PICUP and AUC experiments showed that pre-SAA1.1 and Ser-SAA1.1 form different oligomers. SV-AUC experiment showed that in solution pre-SAA1.1 mainly exists as tetramers and octamers, where Ser-SAA1.1 forms a hexamer. Previous studies have shown that human SAA1.1 exists as a dimer of trimers in crystal structure and in solution[29] and it dissociated to trimers under the treatment of 4 M GdnHCl. The trimeric SAA1.1 is formed mainly by the interaction of helix1 in monomeric SAA1.1 with a head-to-tail packing.[29] Since the SP is a distinct extension at the N-terminus of SAA1.1, it is likely that the steric hindrance from the SP makes pre-SAA1.1 adapt to the formation of the oligomers different from the hexamer formed by SAA1.1. In combination with our results from tertiary structure studies, the more buried tryptophan residues and less exposed hydrophobic surfaces of pre-SAA1.1 likely result from the different oligomeric assemblies.

Our intrinsic fluorescence results showed that the tryptophan residues of pre-SAA1.1 move toward a more hydrophobic environment in comparison with Ser-SAA1.1. This generally keeps the tryptophan residues away from the fluorescence quenching effect of solvent and leads to an increased fluorescence intensity. However, the fluorescence spectrum of pre-SAA1.1 displayed a decrease in the fluorescence intensity compared with Ser-SAA1.1. In our chemical denaturation studies, the similar phenomenon was also observed for both pre-SAA1.1 and Ser-SAA1.1. In the native state (folded state), the spectra of pre-SAA1.1 and Ser-SAA1.1 both showed lower fluorescence intensities than in their unfolded state. The fluorescence quenching in the native state of protein compared with their unfolded state has been reported in other proteins such as γD-crystallin.[50] This effect results from the fact that side chains of amino acid residues can also be quenchers of tryptophan fluorescence as reported by Chen and Barkley.[51] Therefore, native pre-SAA1.1 and Ser-SAA1.1 likely fold into conformations in which their tryptophan residues are located close to the amino acid fluorescence quenchers and the fluorescence is quenched. Unfolding relieves the quenching effect of these amino acids. Similarly, it is likely that the amino acid quenchers are in closer proximity to the tryptophan residues in native pre-SAA1.1 than in Ser-SAA1.1 and thus quench the fluorescence of pre-SAA1.1 to a larger degree.

In our thermal and chemical denaturation studies, we found that the 18-residue SP substantially increased the protein stability of SAA1.1. The increased stability by the presence of the SP further inhibits the amyloidogenicity of SAA1.1, in which pre-SAA1.1 was unable to form amyloid fibrils but Ser-SAA1.1 could. The major protein species found in amyloid depositions of human organs are the C-terminal truncated fragments of SAA1.[52] This is consistent with the finding that the C-terminal tail stabilizes the helix bundle structure of SAA1.1 by forming multiple salt bridges and hydrogen bonds with helix 1, 2, and 4.[29] Deletion of the first 11 residues at N-terminal region in helix 1 resulted in decreased amyloidogenicity of SAA1.[53] The amyloidogenic core of SAA1 was reported to locate at residues ^{2}SFFSFLG^{8} in helix 1 and residues ^{52}VWAAEAIS^{59} in helix 3.[29,54] Since the SP presents in the N-terminal region of SAA1.1, that is close to the

amyloidogenic core, it is possible that the presence of SP in pre-SAA1.1 leads to a more stable structure of SAA1.1 and/or creates a hindrance for fibrillization that further reduces the amyloid formation of SAA1.1. It has been proposed that the helical hexameric SAA1.1 may undergo dissociation to initiate β-sheet formation of amyloid fibrillization.[29] It is also possible that pre-SAA1.1 assembles into more stable oligomers, that is, tetramers and octamers, that cannot dissociate easily to monomer to further prevent fibrillization. Our results showed that the aggregation of Ser-SAA1.1 cannot be inhibited by the addition of the synthetic SP. This further suggests that the inhibitory effect comes from the stabilization of SAA1.1 rather than interactions between the SP and SAA1.1.

There are also some limitations of the present study. First, all our experiments were carried out in vitro and thus it should be acknowledged that the circumstances and the conformational states of SAA1.1 can be different in vivo. At this stage, we do not know the exact structure and assemblies of SAA1.1 in cell or human body. It has been shown that other SAA proteins form different oligomers. Previous crystal structure studies reported that free murine SAA3 forms tetramers[55] whereas murine SAA3 arranges as trimers when bound to retinol.[56] These findings show that the oligomeric states of SAA proteins are not invariable and SAA proteins may arrange into the different assemblies to conduct their function. The biologically-relevant structures and assemblies of SAA1.1 still need further studies to uncover. Since the cleavage of the SP generates mature SAA1.1 during secretion, pre-SAA1.1 may not appear outside the secretory pathway. Even though pre-SAA1.1 is not the functionally relevant species in human body, by using pre-SAA1.1 as a research model, our results demonstrated that amyloid formation may be inhibited by the stabilization of SAA1.1 through targeting its N-terminus.

The current preventative and therapeutic strategy for AA amyloidosis is to suppress the production of SAA by cytokine blockers such as antagonists for IL-1, IL-6, and TNF-α, or by cytotoxic agents and colchicine.[57] Small compounds such as DMSO and eprodisate have also been shown to prevent amyloid formation and applied to AA amyloidosis.[58,59] Besides, peptide inhibitors were designed based on their similarity and complementarity to the N-terminal amyloidogenic region of SAA to inhibit SAA amyloid formation.[60,61] Based on our results, we suggest a potential therapeutic strategy to target the very N-terminus of SAA1 and stabilize the protein that prevents amyloid formation. The increase of protein stability to prevent amyloidosis has been successfully delivered to clinical use in the example of Tafamidis for transthyretin (TTR) in hereditary TTR amyloidosis.[62] The compound stabilizes the tetrameric assembly of TTR and prevents the dissociation and misfolding to amyloid fibrils.[62] Another study for Alzheimer disease has also shown that targeting the N-terminal residues 3–7 of Aβ, which is away from the amyloidogenic core, by N-terminal specific antibodies prevents Aβ aggregation and rescues the detrimental effect in mice.[63] In summary, in the present study we discovered the stabilizing role of SP in SAA and facilitated the therapeutic development for AA amyloidosis.

4 | MATERIALS AND METHODS

4.1 | Protein expression and purification

Human pre-SAA1.1 (with SP) and mature SAA1.1 (without SP) were constructed and cloned into pET-14b vectors between the *Nde*I and *BamH*I sites. Pre-SAA1.1 and SAA1.1 both contained an N-terminal His-tag. A TEV protease cleavage site (ENLYFQS) was added to the N-terminus of SAA1.1 sequence for His-tag removal. After TEV protease cleavage, SAA1.1 retained an additional serine residue at the N-terminus and is referred to as Ser-SAA1.1. The pET-14b vectors were transformed into *E. coli* T7 expression strain BL21 and the transformed cells were grown in LB medium at 37°C until the OD_{600} reached 0.6–0.8. The expression of recombinant proteins was then induced by the addition of 1 mM IPTG. Induction was allowed to proceed for 5 hr, and cells were harvested by centrifugation. The cells containing pre-SAA1.1 were resuspended in 20 mM Tris–HCl buffer, pH 8, 150 mM NaCl, containing protease inhibitor cocktail (Complete, EDTA-free, Roche Applied Science, Germany). To increase solubility, the cells containing Ser-SAA1.1 were resuspended in 20 mM Tris–HCl buffer, pH 8, containing 5 M urea. Resuspended cells were then lysed by a microfluidizer (model M110L, Microfluidics, Westwood, Massachusetts). Pre-SAA1.1 and Ser-SAA1.1 proteins were purified by HisTrap HP column (GE Healthcare Bio-Sciences, Piscataway, New Jersey) on a ÄKTA FPLC system (GE healthcare Bio-Sciences AB, Sweden) in the absence or presence of 5 M urea, respectively. The His-tag was removed from Ser-SAA1.1 by incubation with TEV protease in a TEV:SAA molar ratio of 1:20 at 30°C for 16 hr. Ser-SAA1.1 after TEV protease cleavage was purified by passing through a Histrap column again and collected as the flow-through. The purified pre-SAA1.1 and Ser-SAA1.1 proteins were concentrated and dialyzed into a fresh 50 mM phosphate buffer, pH 7.0, and stored in aliquots at −80°C for subsequent experiments.

4.2 | Synthesis and preparation of the SP of SAA1.1

The SP of SAA1.1 was chemically synthesized and purchased from Scientific Biotech Corp. (Taipei, Taiwan). The peptide sequence is MKLLTGLVFCSLVLGVSS. The SP stock was freshly prepared prior to the experiments by dissolving the lyophilized SP in 10 μl of dimethyl sulfoxide (DMSO), then diluting 10-fold into a 50 mM phosphate buffer, pH 7.0. The dissolved SP was centrifuged at 17,000*g* at 4°C for 10 min to remove possible precipitates and quantified using a Pierce BCA Protein Assay kit (Thermo Fisher Scientific, Waltham, Massachusetts).

4.3 | Far-UV CD

The protein samples were prepared at a final concentration of 20 μM in 50 mM phosphate buffer, pH 7.0, then subjected to Far-UV CD measurement. Far-UV CD spectra were examined by a Jasco J-815 spectropolarimeter (Jasco Co., Japan) with a 1-mm path length quartz cuvette (Hellma, Germany) at 4°C. The spectra were acquired over a wavelength range of 190–250 nm at a scan rate of 100 nm/min. Data was collected as an average of 10 scans with 1 nm bandwidth. Averaged CD signals, corrected with buffer background, were converted to mean residue ellipticity [Θ] (deg cm^2 $dmol^{-1}$) according to the equation:

$$[\Theta] = (100\theta)/(Cnl)$$

where, θ is the measured ellipticity (millidegrees, mdeg), C is the protein concentration (mM), n is the number of amino acid residues, and l is the path length (cm).

4.4 | Intrinsic fluorescence spectroscopy

Fluorescence spectroscopy measurements were conducted on a FluoroMax Plus spectrofluorometer (Horiba Jobin Yvon Inc., Edison, New Jersey) at room temperature using a quartz cuvette of 3-mm path length (Hellma). The excitation wavelengths were 280 and 295 nm and the emission spectra were recorded from 300 to 450 nm. The slit widths for excitation and emission were 2 and 1.5 nm, respectively. The final spectra were averaged over 3 scans and the buffer background were subtracted.

4.5 | ANS fluorescence

ANS stock solution was prepared to a concentration of 20 mM in a 50 mM phosphate buffer, pH 7.0. Each sample contained 20 μM of pre-SAA1.1 or Ser-SAA1.1 proteins and a final concentration of 200 μM ANS. ANS was allowed to interact with any exposed hydrophobic patches of the proteins at room temperature for 1 hr. The fluorescence of ANS was excited at 375 nm and the emission spectra were recorded from 390 to 600 nm. Both excitation and emission slit widths were 2 nm. Each final spectrum was an average of 3 scans and the buffer background were subtracted.

4.6 | PICUP

Photo-induced crosslinking of pre-SAA1.1 and Ser-SAA1.1 was performed following previous literature.[64] Briefly, the stock solutions of 1 mM Tris(2,2′-bipyridyl) dichlororuthenium(II) hexahydrate ($Ru(bpy)_3Cl_2$) and 20 mM ammonium persulfate (APS) were freshly prepared in 10 mM sodium phosphate buffer, pH 7.4, respectively. Each sample for PICUP included 18 μl of 20 μM pre-SAA1.1 or Ser-SAA1.1 protein, 1 μl of $Ru(bpy)_3Cl_2$ stock, and 1 μl of APS stock. The samples were irradiated with a blue LED light for 1, 5, 10, and 30 s and quenched immediately by the addition of SDS-PAGE sample buffer containing β-mercaptoethanol. The samples were then boiled at 95°C for 10 min. The controls were prepared under the same conditions except the addition of crosslinking reagents or light exposure as indicated. The crosslinked samples were further analyzed by western blot with an anti-SAA antibody (ab687, Abcam, Cambridge, Massachusetts).

4.7 | Analytical ultracentrifugation

Sedimentation velocity (SV) experiments were performed on a ProteomeLab XL-I analytical ultracentrifuge (Beckman Coulter, Brea, California). Each sample containing 20 μM protein in 50 mM phosphate buffer, pH 7.0, was loaded into a double-sector cell with a 12-mm Epon centerpiece. Data was collected at 25,000 rpm using an An-60 Ti rotor at 4°C and the radial position of protein molecules was detected by UV absorbance at 275 nm. The SV absorbance profiles were analyzed by SEDFIT software using a continuous [$c(s)$] distribution model to obtain the apparent distribution of sedimentation coefficients (s).

4.8 | Thermal denaturation

The temperature melting and cooling of pre-SAA1.1 and Ser-SAA1.1 at 20 μM were performed at pH 7.0 on a Jasco

J-815 spectropolarimeter using a PTC 423 S/15 Peltier temperature controller (Jasco Co.). The protein samples in a rectangular quartz cuvette (1-mm path length, Hellma) were heated from 4°C to 100°C and then cooled from 100°C to 4°C at a rate of 2°C/min and the structural changes were monitored by CD ellipticity (mdeg) at 222 nm. Data was collected at an interval of 2°C with a bandwidth of 1 nm. The fraction of the unfolded protein (f_U) was calculated using the following equation:

$$f_U = (y_{\text{obs}} - y_{4^\circ\text{C}})/(y_{100^\circ\text{C}} - y_{4^\circ\text{C}})$$

where y_{obs} is the observed CD signal at any temperature along the denaturation; $y_{4^\circ\text{C}}$ and $y_{100^\circ\text{C}}$ are the signals observed at 4°C and 100°C, respectively.

4.9 | ThT assay

Pre-SAA1.1 and Ser-SAA1.1 were dialyzed into a freshly-prepared 50 mM phosphate buffer, pH 7.0, centrifuged at 17,000*g* at 4°C for 10 min to remove possible precipitates, and re-quantified. Samples were prepared with 20 μM proteins and 10 μM ThT. After preparation, the samples were transferred into a 384-well opaque microplate and sealed with a transparent film. Fibrillization of pre-SAA1.1 and Ser-SAA1.1 was monitored by the ThT fluorescence measured at 25°C every 30 min with a 40 s agitation prior to the measurement. ThT fluorescence was excited at 442 nm, and the emission was collected at 485 nm by software SoftMax Pro 6.3 in SpectraMax M3 microplate reader (Molecule Devices, San Jose, California).

4.10 | Transmission electron microscopy

The end-point products acquired from ThT assay were subjected to TEM imaging. Ten microliters of ThT assay end-point products were placed on glow-discharged, 400-mesh Formvar carbon-coated copper grids (EMS Inc., Hatfield, Pennsylvania) for 10 min, rinsed by double-distilled water, and stained with 1% uranyl acetate for 30 s. The samples were then examined by Tecnai G2 Spirit TWIN TEM (FEI Company, Hillsboro, Oregon) with an accelerating voltage of 120 kV.

AUTHOR CONTRIBUTIONS

Jin-Lin Wu: Data curation (lead); formal analysis (lead); methodology (lead); project administration (lead); writing – original draft (lead). **Yun-Ru Chen:** Conceptualization (lead); funding acquisition (lead); project administration (supporting); supervision (lead); writing – review and editing (lead).

ACKNOWLEDGMENTS

The authors thank the Academia Sinica Biological Electron Microscopy Core Facility for EM technical support. The core facility is funded by the Academia Sinica Core Facility and Innovative Instrument Project (AS-CFII-108-119).

CONFLICT OF INTEREST

The authors have no conflict of interest to declare.

DATA AVAILABILITY STATEMENT

Data are available upon request.

ORCID

Yun-Ru Chen https://orcid.org/0000-0002-6596-6338

REFERENCES

1. Schatz PJ, Beckwith J. Genetic analysis of protein export in escherichia coli. Annu Rev Genet. 1990;24:215–248.
2. Walter P, Johnson AE. Signal sequence recognition and protein targeting to the endoplasmic reticulum membrane. Annu Rev Cell Biol. 1994;10:87–119.
3. von Heijne G. Signal sequences. The limits of variation. J Mol Biol. 1985;184:99–105.
4. von Heijne G. Towards a comparative anatomy of n-terminal topogenic protein sequences. J Mol Biol. 1986;189:239–242.
5. von Heijne G. The signal peptide. J Membr Biol. 1990;115:195–201.
6. Benham AM. Protein secretion and the endoplasmic reticulum. Cold Spring Harb Perspect Biol. 2012;4:a012872.
7. Shao S, Hegde RS. A calmodulin-dependent translocation pathway for small secretory proteins. Cell. 2011;147:1576–1588.
8. Paetzel M, Karla A, Strynadka NC, Dalbey RE. Signal peptidases. Chem Rev. 2002;102:4549–4580.
9. Liu G, Topping TB, Randall LL. Physiological role during export for the retardation of folding by the leader peptide of maltose-binding protein. Proc Natl Acad Sci U S A. 1989;86:9213–9217.
10. Park S, Liu G, Topping TB, Cover WH, Randall LL. Modulation of folding pathways of exported proteins by the leader sequence. Science. 1988;239:1033–1035.
11. Beena K, Udgaonkar JB, Varadarajan R. Effect of signal peptide on the stability and folding kinetics of maltose binding protein. Biochemistry. 2004;43:3608–3619.
12. Kulothungan SR, Das M, Johnson M, Ganesh C, Varadarajan R. Effect of crowding agents, signal peptide, and chaperone secb on the folding and aggregation of *E. COLI* maltose binding protein. Langmuir. 2009;25:6637–6648.
13. Singh P, Sharma L, Kulothungan SR, et al. Effect of signal peptide on stability and folding of escherichia coli thioredoxin. PLoS One. 2013;8:e63442.
14. Feeney B, Clark AC. Reassembly of active caspase-3 is facilitated by the propeptide. J Biol Chem. 2005;280:39772–39785.

15. Pop C, Chen YR, Smith B, et al. Removal of the pro-domain does not affect the conformation of the procaspase-3 dimer. Biochemistry. 2001;40:14224–14235.
16. Yokoi K, Shih LC, Kobayashi R, et al. Serum amyloid a as a tumor marker in sera of nude mice with orthotopic human pancreatic cancer and in plasma of patients with pancreatic cancer. Int J Oncol. 2005;27:1361–1369.
17. Chan DC, Chen CJ, Chu HC, et al. Evaluation of serum amyloid a as a biomarker for gastric cancer. Ann Surg Oncol. 2007; 14:84–93.
18. Wood SL, Rogers M, Cairns DA, et al. Association of serum amyloid a protein and peptide fragments with prognosis in renal cancer. Br J Cancer. 2010;103:101–111.
19. Toriola AT, Cheng TY, Neuhouser ML, et al. Biomarkers of inflammation are associated with colorectal cancer risk in women but are not suitable as early detection markers. Int J Cancer. 2013;132:2648–2658.
20. Biaoxue R, Hua L, Wenlong G, Shuanying Y. Increased serum amyloid a as potential diagnostic marker for lung cancer: A meta-analysis based on nine studies. BMC Cancer. 2016;16:836.
21. Wu JL, Su TH, Chen PJ, Chen YR. Acute-phase serum amyloid a for early detection of hepatocellular carcinoma in cirrhotic patients with low afp level. Sci Rep. 2022;12:5799.
22. Coetzee GA, Strachan AF, van der Westhuyzen DR, Hoppe HC, Jeenah MS, de Beer FC. Serum amyloid a-containing human high density lipoprotein 3. Density, size, and apolipoprotein composition. J Biol Chem. 1986;261:9644–9651.
23. De Buck M, Gouwy M, Wang JM, et al. Structure and expression of different serum amyloid a (saa) variants and their concentration-dependent functions during host insults. Curr Med Chem. 2016;23:1725–1755.
24. Zhang Y, Zhang J, Sheng H, Li H, Wang R. Acute phase reactant serum amyloid a in inflammation and other diseases. Adv Clin Chem. 2019;90:25–80.
25. Liepnieks JJ, Kluve-Beckerman B, Benson MD. Characterization of amyloid a protein in human secondary amyloidosis: The predominant deposition of serum amyloid a1. Biochim Biophys Acta. 1995;1270:81–86.
26. Röcken C, Shakespeare A. Pathology, diagnosis and pathogenesis of aa amyloidosis. Virchows Arch. 2002;440:111–122.
27. Sack GH Jr. Serum amyloid a (saa) proteins. Subcell Biochem. 2020;94:421–436.
28. Sipe JD, Colten HR, Goldberger G, et al. Human serum amyloid a (saa): Biosynthesis and postsynthetic processing of presaa and structural variants defined by complementary DNA. Biochemistry. 1985;24:2931–2936.
29. Lu J, Yu Y, Zhu I, Cheng Y, Sun PD. Structural mechanism of serum amyloid a-mediated inflammatory amyloidosis. Proc Natl Acad Sci U S A. 2014;111:5189–5194.
30. Wang Y, Srinivasan S, Ye Z, Javier Aguilera J, Lopez MM, Colón W. Serum amyloid a 2.2 refolds into a octameric oligomer that slowly converts to a more stable hexamer. Biochem Biophys Res Commun. 2011;407:725–729.
31. Louis-Jeune C, Andrade-Navarro MA, Perez-Iratxeta C. Prediction of protein secondary structure from circular dichroism using theoretically derived spectra. Proteins. 2012;80:374–381.
32. Semisotnov GV, Rodionova NA, Razgulyaev OI, Uversky VN, Gripas AF, Gilmanshin RI. Study of the "molten globule" intermediate state in protein folding by a hydrophobic fluorescent probe. Biopolymers. 1991;31:119–128.
33. Chen YR, Glabe CG. Distinct early folding and aggregation properties of alzheimer amyloid-beta peptides abeta40 and abeta42: Stable trimer or tetramer formation by abeta42. J Biol Chem. 2006;281:24414–24422.
34. Chen WT, Liao YH, Yu HM, Cheng IH, Chen YR. Distinct effects of Zn2+, Cu2+, Fe3+, and Al3+ on amyloid-beta stability, oligomerization, and aggregation: Amyloid-beta destabilization promotes annular protofibril formation. J Biol Chem. 2011;286:9646–9656.
35. Bitan G, Kirkitadze MD, Lomakin A, Vollers SS, Benedek GB, Teplow DB. Amyloid beta -protein (abeta) assembly: Abeta 40 and abeta 42 oligomerize through distinct pathways. Proc Natl Acad Sci U S A. 2003;100:330–335.
36. Maji SK, Ogorzalek Loo RR, Inayathullah M, et al. Amino acid position-specific contributions to amyloid beta-protein oligomerization. J Biol Chem. 2009;284:23580–23591.
37. Rosensweig C, Ono K, Murakami K, Lowenstein DK, Bitan G, Teplow DB. Preparation of stable amyloid β-protein oligomers of defined assembly order. Methods Mol Biol. 2012;849:23–31.
38. Sugiki T, Utsunomiya-Tate N. Site-specific aspartic acid isomerization regulates self-assembly and neurotoxicity of amyloid-β. Biochem Biophys Res Commun. 2013;441:493–498.
39. Jana MK, Cappai R, Pham CL, Ciccotosto GD. Membrane-bound tetramer and trimer aβ oligomeric species correlate with toxicity towards cultured neurons. J Neurochem. 2016;136: 594–608.
40. Naiki H, Higuchi K, Hosokawa M, Takeda T. Fluorometric determination of amyloid fibrils in vitro using the fluorescent dye, thioflavin t1. Anal Biochem. 1989;177:244–249.
41. Biancalana M, Koide S. Molecular mechanism of thioflavin-t binding to amyloid fibrils. Biochim Biophys Acta. 2010;1804: 1405–1412.
42. Real de Asúa D, Costa R, Galván JM, Filigheddu MT, Trujillo D, Cadiñanos J. Systemic aa amyloidosis: Epidemiology, diagnosis, and management. Clin Epidemiol. 2014;6: 369–377.
43. Rodriguez FJ, Picken MM, Lee JM. Amyloid deposition in the central nervous system. In: Picken MM, Herrera GA, Dogan A, editors. Amyloid and related disorders: Surgical pathology and clinical correlations. Cham: Springer International Publishing, 2015; p. 121–131.
44. Benson MD, Buxbaum JN, Eisenberg DS, et al. Amyloid nomenclature 2020: Update and recommendations by the International Society of Amyloidosis (ISA) nomenclature committee. Amyloid. 2020;27:217–222.
45. Nuvolone M, Merlini G. Systemic amyloidosis: Novel therapies and role of biomarkers. Nephrol Dial Transplant. 2017;32: 770–780.
46. Pinney JH, Lachmann HJ. Systemic aa amyloidosis. Subcell Biochem. 2012;65:541–564.
47. Dubrey SW, Cha K, Simms RW, Skinner M, Falk RH. Electrocardiography and doppler echocardiography in secondary (aa) amyloidosis. Am J Cardiol. 1996;77:313–315.
48. Hassan W, Al-Sergani H, Mourad W, Tabbaa R. Amyloid heart disease. New frontiers and insights in pathophysiology, diagnosis, and management. Tex Heart Inst J. 2005;32:178–184.

49. Tanaka F, Migita K, Honda S, et al. Clinical outcome and survival of secondary (aa) amyloidosis. Clin Exp Rheumatol. 2003; 21:343–346.
50. Kosinski-Collins MS, Flaugh SL, King J. Probing folding and fluorescence quenching in human gammad crystallin greek key domains using triple tryptophan mutant proteins. Protein Sci. 2004;13:2223–2235.
51. Chen Y, Barkley MD. Toward understanding tryptophan fluorescence in proteins. Biochemistry. 1998;37:9976–9982.
52. Westermark GT, Fändrich M, Westermark P. Aa amyloidosis: Pathogenesis and targeted therapy. Annu Rev Pathol. 2015;10: 321–344.
53. Patel H, Bramall J, Waters H, De Beer MC, Woo P. Expression of recombinant human serum amyloid a in mammalian cells and demonstration of the region necessary for high-density lipoprotein binding and amyloid fibril formation by site-directed mutagenesis. Biochem J. 1996;318(Pt 3):1041–1049.
54. Rubin N, Perugia E, Wolf SG, Klein E, Fridkin M, Addadi L. Relation between serum amyloid a truncated peptides and their suprastructure chirality. J Am Chem Soc. 2010;132:4242–4248.
55. Derebe MG, Zlatkov CM, Gattu S, et al. Serum amyloid a is a retinol binding protein that transports retinol during bacterial infection. Elife. 2014;3:e03206.
56. Hu Z, Bang YJ, Ruhn KA, Hooper LV. Molecular basis for retinol binding by serum amyloid a during infection. Proc Natl Acad Sci U S A. 2019;116:19077–19082.
57. Pettersson T, Konttinen YT, Maury CP. Treatment strategies for amyloid a amyloidosis. Expert Opin Pharmacother. 2008;9: 2117–2128.
58. Amemori S, Iwakiri R, Endo H, et al. Oral dimethyl sulfoxide for systemic amyloid a amyloidosis complication in chronic inflammatory disease: A retrospective patient chart review. J Gastroenterol. 2006;41:444–449.
59. Dember LM, Hawkins PN, Hazenberg BP, et al. Eprodisate for the treatment of renal disease in aa amyloidosis. N Engl J Med. 2007;356:2349–2360.
60. Sosnowska M, Skibiszewska S, Kamińska E, Wieczerzak E, Jankowska E. Designing peptidic inhibitors of serum amyloid a aggregation process. Amino Acids. 2016;48:1069–1078.
61. Skibiszewska S, Żaczek S, Dybala-Defratyka A, Jędrzejewska K, Jankowska E. Influence of short peptides with aromatic amino acid residues on aggregation properties of serum amyloid a and its fragments. Arch Biochem Biophys. 2020;681:108264.
62. Bulawa CE, Connelly S, Devit M, et al. Tafamidis, a potent and selective transthyretin kinetic stabilizer that inhibits the amyloid cascade. Proc Natl Acad Sci U S A. 2012;109:9629–9634.
63. Basi GS, Feinberg H, Oshidari F, et al. Structural correlates of antibodies associated with acute reversal of amyloid beta-related behavioral deficits in a mouse model of alzheimer disease. J Biol Chem. 2010;285:3417–3427.
64. Vollers SS, Teplow DB, Bitan G. Determination of peptide oligomerization state using rapid photochemical crosslinking. Methods Mol Biol. 2005;299:11–18.
65. Eisenberg D, Schwarz E, Komaromy M, Wall R. Analysis of membrane and surface protein sequences with the hydrophobic moment plot. J Mol Biol. 1984;179:125–142.

SUPPORTING INFORMATION

Additional supporting information can be found online in the Supporting Information section at the end of this article.

How to cite this article: Wu J-L, Chen Y-R. Signal peptide stabilizes folding and inhibits misfolding of serum amyloid A. Protein Science. 2022;31(12):e4485. https://doi.org/10.1002/pro.4485